Size exclusion and diffusion of fluoresceinated probes within collagen fibrils

A. Ekani-Nkodo and D. Kuchnir Fygenson*
Physics Department, University of California, Santa Barbara, California 93106
(Received 15 October 2002; published 21 February 2003)

The diffusion of fluoresceinated probes inside single collagen fibrils was investigated by imaging the migration of fluorescence along the fibrils in oil and by monitoring fluorescence recovery after photobleaching (FRAP). Probes were excluded from the fibrils according to their size. Probes that were not excluded diffused in the fibrils, but FRAP occurred 6×10^{-4} times more slowly than in water due to binding interactions between collagen and the probes. The dissociation constant of the fluorescein-collagen complex was determined ($K_D=1.8\pm0.1\ \mu$M).

DOI: 10.1103/PhysRevE.67.021909 PACS number(s): 87.15.Vv, 87.16.Ka, 87.64.Rr, 87.14.Ee

I. INTRODUCTION

Collagen fibrils are one of the most important components of animal tissue, pervading a wide variety of extracellular environments, such as bones, tendons, or ligaments. Collagen accounts for a tissue's mechanical properties [1,2] and, therefore, understanding its structure and biochemistry is crucial for the development of new therapies [3]. However, although many works have investigated the formation and structure of collagen fibrils, a definite picture has yet to emerge. Different models have been proposed, ranging from long-range ordered (crystal) to disordered (liquid) to a combination of both.

Fibrillar collagen are rodlike molecules about 300 nm in length and about 1.5 nm in diameter [4]. They assemble into cylindrical fibrils that range from 10 to 500 nm in diameter [5], depending on the age and type of collagen. The concentration of collagen in the fibrils is around 4 mM [4]. From electron microscopy (EM) [6,7] and x-ray diffraction [8], a molecular organization was suggested with molecules staggered axially to create *a* of 67 nm banding. This banding is also observed in atomic force microscopy images [9,10]. The lateral arrangement, however, is not as well determined. Using x-ray diffraction, Hulmes *et al.* [11,12] made observations consistent with a quasihexagonal packing, while other studies show liquidlike order [13–15]. Accordingly, lateral spacings ranging from about 1.1 to 4 nm were reported [7,16].

Recently, surprising evidence for lateral inhomogeneity in the structure of individual collagen fibrils has emerged [17]. From atomic force microscopy (AFM) measurement and fibril manipulation using micropipettes, it was observed that collagen fibrils collapse in a tubelike manner. This suggests that collagen molecules are more heavily cross-linked in an outer region (shell) and more fluid in the inner region (core) of a fibril.

It is natural to wonder if this tubelike character extends to transport as well as mechanical properties of collagen fibrils. The study of transport properties inside collagen fibrils should further illuminate their structure and may also be relevant to biological processes.

One way to probe the inner structure of a ''tubelike'' material is to measure the diffusion coefficient of molecules of different size during their migration inside the material. In this vein, we undertook to determine the translational diffusion of small fluorescent molecules in collagen fibrils by fluorescence recovery after photobleaching (FRAP). Although this technique has less spatial resolution than imaging techniques like AFM or x-ray diffraction, it can provide dynamic information on anisotropy, free volume, and viscosity. In the case of collagen fibrils, technical challenges arise due to the severe aspect ratio of the fibrils and the extraordinary stickiness of collagen.

Studies of diffusion in microscopic fibers are relatively rare. Rattee and So [18] measured the diffusion of radioactive tracer in polyamide (nylon 66) fibers a few tens of microns in diameter. Song *et al.* [19] also studied diffusion in nylon 66 fibers. They used a laser scanning confocal microscope to measure the radial diffusion of fluorescein. As for biological fibers, Papadopoulos *et al.* [20] studied protein diffusion in living skeletal muscle fiber bundles (10–100 μm). And our group recently conducted a study of diffusion of a reversibly binding ligand in microtubule bundles (1–10 μm) [21]. Here we report the feasibility of measuring diffusion in single biological fibers <500 nm in diameter using a simple experimental FRAP setup.

II. MATERIALS AND METHODS

A. Sample preparation

For all solutions prepared for imaging, the buffer was PBS (pH=7.4, Sigma) with 2 mM sodium azide. Fluorescein was purchased from Sigma (Acid Yellow) and hydrated to a final concentration of 5 mg/ml (15 mM). Fluoresceinated dextran of mean molecular weight $M_w=1500$ and $M_w=8800$ (Molecular Probes), hereafter referred to as 3 kD and 10 kD dextran, respectively (following the manufacturer's denomination), were hydrated to a concentration of 50 mg/ml (33 nM and 6 mM, respectively). Tendons were extracted from tails of mature rats sacrificed for other experiments. Tails were stored frozen for several weeks before the experiment.

For samples imaged in aqueous solution, thawed tendons were immersed in dye solution overnight at 4 °C. Once stained, tendons were shredded in a Petri dish containing

*To whom correspondence should be addressed. Electronic mail: deborah@physics.ucsb.edu

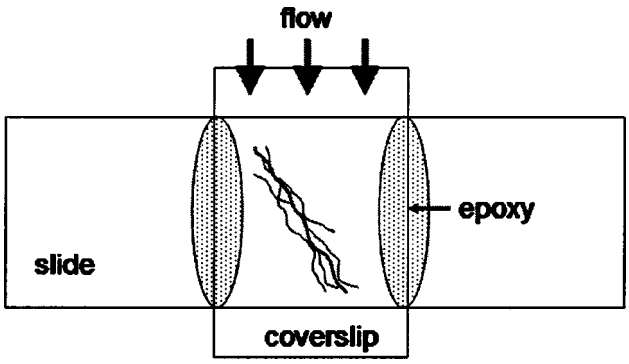

FIG. 1. Flow cell used for FRAP measurements. The coverslip is glued to the slide on two sides with epoxy. The two other sides are left open. Buffer is applied to one side with a pipettor and sucked out the other using a kimwipe.

PBS and left soaking for 1 h. This process removed dye trapped between fibrils and was crucial for imaging. Soaked fibrils were gently spread on a microscope slide and covered with a coverslip larger than the slide (Fig. 1). The sample was then sealed on two sides with epoxy. This left a flow path that was accessible during observation on an inverted microscope (Fig. 2). The sample was rinsed by applying dye-free buffer to one of the open ends of the coverslip with a pipettor and withdrawing from the other using a kimwipe.

For samples imaged in oil, thawed tendons were dissected into fiber bundles, which were then spread onto a standard microscope slide. One end of a fiber bundle was covered in a drop of mineral oil (Fisher Scientific) and the other in a drop of fluorescein or fluoresceinated dextran in PBS. The bundle was then covered with a coverslip and sealed with epoxy. After a few hours, fibrils in the oil region could be seen by fluorescence.

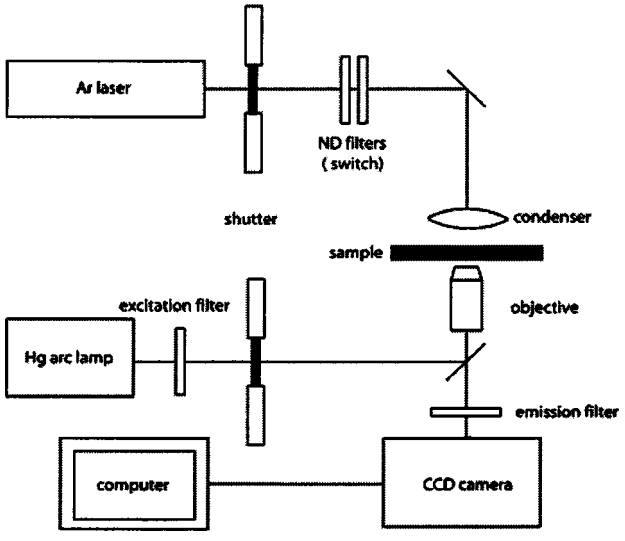

FIG. 2. Schematic of the FRAP experimental setup. The same laser beam is used to bleach (neutral density off) and to monitor the recovery of intensity (neutral density on). The arc lamp is only used to visualize the whole sample. The objective is a 100×/1.35 NA oil immersion.

B. FRAP setup

The FRAP setup consisted of an inverted microscope (IX 70, Olympus) coupled to a 25-mW argon ion laser (Ion Laser Technology) (Fig. 2). Blue light (488 nm) from the bottom arc lamp was used to visualize the whole sample and locate single collagen fibrils. Then the laser beam, focused from above through a low-power 0.9 NA condenser (Olympus), was positioned on the fibril of choice. Observations were performed with a 100×/1.35 NA oil objective. The emitted fluorescence passed through a dichroic mirror and an interference filter (560 ± 60 nm). Images were recorded directly to computer RAM via a CCD (1310 camera, DVC) and a frame grabber (Pixci, Epix) using the software control package XCAP (Epix).

In reading mode, the laser power was set on low (3 mW) and two neutral density filters attenuated the beam. In bleach mode, the laser power was set on high (25 mW) and the neutral density filters were removed. The spot was Gaussian with a width of 5 μm. By measuring with a power meter the intensity of the laser beam at the sample position, the power used for bleaching was found to be roughly 2×10^3 times greater than for reading. Switching between modes required 1 s, which was fast compared to the time scale of fluorescence recovery observed.

As a control, FRAP measurements were performed on fluorescein and fluoresceinated 3 kD dextran freely diffusing in a solution of 80% glycerol (Acros) in water at a concentration of 66 and 25 μM, respectively. The viscosity of this solution was approximately 60 times greater than that of water [22]. The high viscosity slowed diffusion enough that integration times of 0.25—1 s could be used. With shorter integration times, the detected intensity was low and experimental signals were noisy.

All experiments were carried out at room temperature.

C. Image acquisition and data analysis

Before imaging, samples were rinsed with 0.5–1 ml (25–50 times the cell volume) of PBS in the flow cell until the background became dark compared to the fibrils. Then a fibril of interest was illuminated with the laser beam and bleached while images were recorded by the computer.

To limit photobleaching during observation, a shutter let the beam through only during image acquisition, which was about 1/3 of the total observation time (600–1200 s). The intensity of nonbleached samples was constant over the observation time under all conditions. Thus photobleaching during recovery was negligible. Reversible recovery of photobleached molecules was also ignorable since the associated time scales are typically on the order of milliseconds [23]. For measurements on collagen fibrils, typical integration times and capture intervals were 2.5 and 7.5 s, respectively, with fluorescein and 4 and 12 s with fluoresceinated dextran. In glycerol, the total observation time was 10 times shorter (60–120 s) and the integration time ranged from 0.25 to 2 s.

The total intensity of the region of interest was integrated for each image and then plotted against time. In glycerol and collagen samples, all curves were best fit to a biexponential decay. But deriving the diffusion coefficient from any of the

times scales obtained from the fits is not straightforward [24,25]. Instead, results were compared to those obtained from a sample of known viscosity [24]. Following Kao, Abney, and Verkman, $t_{1/2}$ was determined from

$$I(t_{1/2}) = \frac{I(0)+I(\infty)}{2}, \tag{1}$$

where $I(0)$ is the intensity measured from the first frame after the bleach and $I(\infty)$ is the plateau value at long time. Kao *et al.* showed that in solution, $t_{1/2}$ can be used as a single parameter to characterize the recovery rate.

D. Measurements of the dissociation constant

Purified collagen in 50 mM acetic acid solution was purchased from Chondrex. This type-I collagen was extracted and purified from rat skin and was not chemically modified. It was diluted to a final concentration of 750 nM in solutions of fluoresceinated probes. The concentration of probes ranged from 0.732 to 750 nM. An identical sets of samples without collagen were used as reference solutions. Both sets were filtered through 5000 NMWL (10 000 NMWL for 3 kD dextran) centrifugational filters (Millipore) for 30 min at 14 000×g. The probe concentration of the filtrate was determined from fluorescence measured with a Cary Eclipse fluorescence spectrophometer (Varian, Inc.).

III. RESULTS AND DISCUSSION

Diffusion of a probe in a crowded medium is different from that in free solution. Steric interactions (less free volume available) and frictional interactions become important when the size of the probe is comparable to the size of interstices. In addition, if the probe has an affinity for the matrix, its overall mobility will be substantially diminished because of repeated binding events.

The collagen fibril is a crowded medium. Here we quantify the effect of binding and steric hindrance on nanometer-sized fluoresceinated probes and report the extent to which their diffusion in fibrils differs from free solution.

A. Dissociation constant

The binding between collagen and fluorescein molecules can be described as a chemical reaction

$$C + nF \leftrightarrow CF_n, \tag{2}$$

where C and F are the collagen and free fluorescein concentrations, respectively, while CF_n is the collagen-fluorescein complex, of uncertain stoichiometry n. The equilibrium constant is defined by

$$K_{\mathrm{eq}} = \frac{CF_n}{F^n C}, \tag{3}$$

and the dissociation constant can be expressed as

$$K_D = \frac{nR^n}{1-R} C_0 F_0^{n-1} - R^n F_0^n, \tag{4}$$

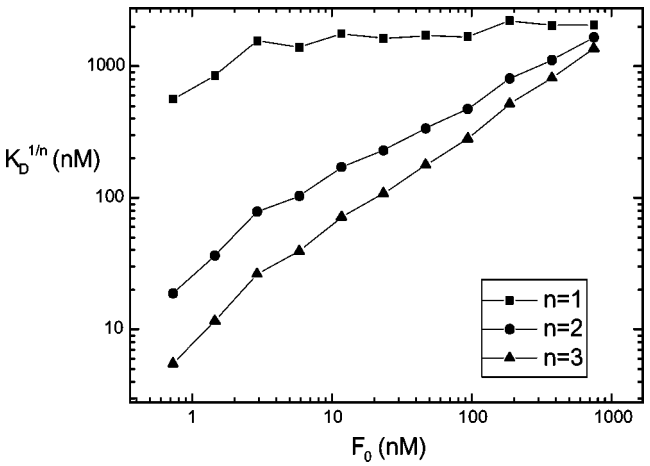

FIG. 3. Dissociation constant of the fluorescein-collagen complex measured at different values of the total fluorescein concentration F_0 [Eq. (4)]. The total collagen concentration C_0 is 750 nM, K_D is independent of F_0 only for a stoechiometry of 1:1 ($n=1$).

where C_0 and F_0 (determined from the reference solutions) are the total concentrations of collagen and fluorescein and $R=F/F_0$ is the fraction of fluorescein left in solution at equilibrium. Thus the dissociation constant can be determined by measuring R.

In Fig. 3, we plot $K_D^{1/n}$ versus F_0 with $C_0=750$ nM for three different stoichiometries: $n=1$, $n=2$, and $n=3$. It is clear that K_D is consistent only for $n=1$, meaning a stoichiometry of 1:1. The average value obtained is then $K_D=1.8 \pm 0.1\ \mu$M. The same experiment performed with 3 kD dextran (data not shown) yielded $K_D=1.7\pm 0.3\ \mu$M.

We conclude that fluorescein binds collagen strongly and suggest that the presence of dextran does not alter the kinetic constants of binding.

B. Size exclusion

In an attempt to force dye to travel inside fibrils along their axis, we immersed one end of a fibril in an oil droplet and the other in a drop of dye solution (see Methods). With fluorescein, the part of the fibril immersed in oil was fluorescent after a few hours [Fig. 4(a)]. However, with 3 kD or 10 kD dextran [Fig. 4(b)], fibrils remained dark for days, but were surrounded by a bright region within several hours.

The bright region is evidently a water layer through which the dye diffuses more readily. The failure of oil to wet the fibril is likely due to hydrophilic proteoglycans that are known to decorate the fibril surface. This layer was not seen in the experiment with fluorescein because fibrils were more heavily stained and therefore imaged with a shorter integration time.

This straightforward approach to characterizing transport down the core of a collagen fibril is therefore foiled by the existence of a short circuit through this hydration layer. It nevertheless points to a size effect. Contrary to fluorescein, many fluoresceinated dextran molecules are excluded from the fibrils.

In accordance with the strong affinity measured above, fibrils stained by immersion in aqueous solution of fluores-

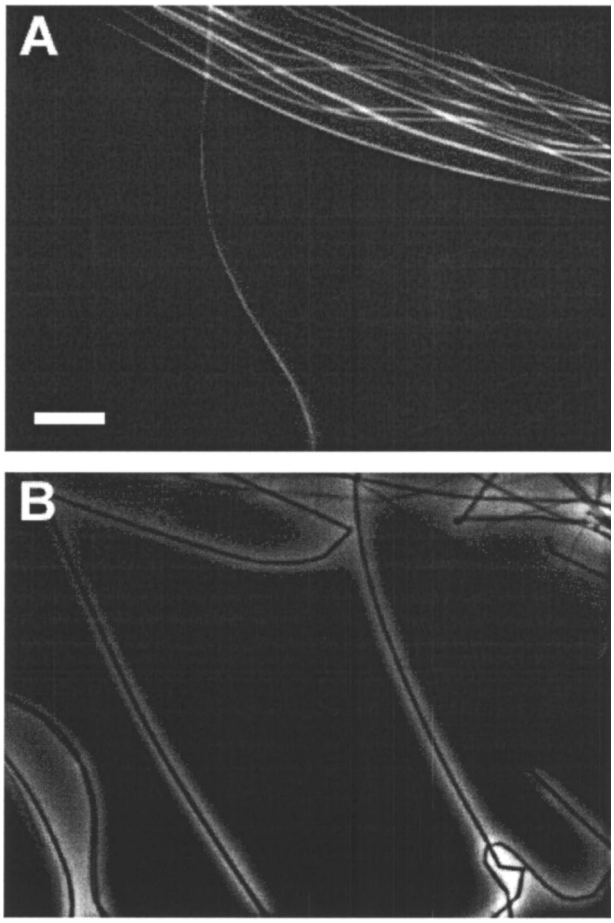

FIG. 4. Oil experiment (see text). With fluorescein: dye stains the fibrils (variations of intensity along a fibril are due to changes of focal plane). With 10 kD dextran: dye stays outside the fibrils, which then appear darker than the surrounding water layer. The scale bar is 5 μm.

cent probes retained fluorescence despite extensive rinsing. Without rinsing, we noted that fibrils immersed in fluorescein were brighter than the background, indicating that dye accumulated inside them, while fibrils immersed in fluoresceinated dextran were darker than (10 kD dextran) or as bright as the background (3 kD dextran).

After rinsing until the background appeared dark, fibrils that had been immersed in 3 kD dextran could be imaged in fluorescence (Fig. 5) while fibrils that had been immersed in 10 kD dextran never developed sufficient contrast. Given their identical binding affinities reported above, we conclude that higher molecular weight dyes are preferentially excluded from the fibrils based on size alone.

Assuming a quasihexagonal molecular packing of collagen molecules, the size of the interstices in a fibril is an estimated $2r=1.3$ nm [12]. It is interesting to compare this value to the hydrodynamic radius of our probes. The Mark-Houwink equation relates the intrinsic viscosity $[\eta]$ of a polymer to its molecular mass M_w:

$$[\eta]=KM_w^{\alpha}, \tag{5}$$

where K and α are constants determined experimentally for a

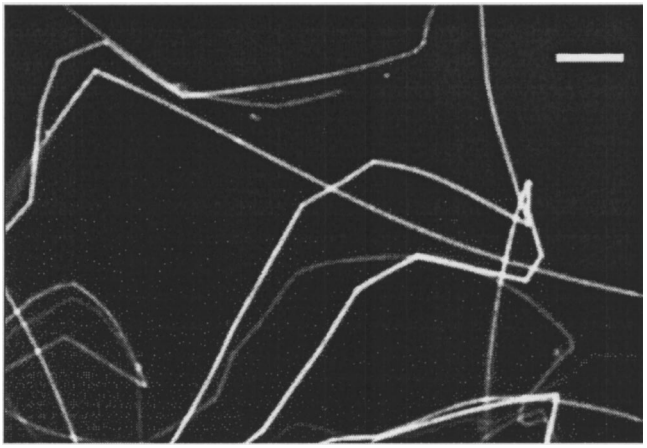

FIG. 5. Collagen fibrils stained with 3 kD dextran after rinse. Before the rinse, fibrils were barely distinguishable from the background. After rinsing, they are easily seen by fluorescence. The scale bar is 5 μm.

wide number of polymers and range of molecular weights. Using the theory of polymer solutions [26], the radius of gyration R_g is

$$R_g=\left(\frac{[\eta]M_W}{6.2N_a}\right)^{1/3}, \tag{6}$$

where N_a is the Avogadro number. The hydrodynamic radius R_h is defined in terms of the diffusion coefficient, which is related to the radius of gyration [27]:

$$D=\frac{kT}{6\pi\eta_s R_h}=\frac{0.203kT}{\sqrt{6}\,\eta_s R_g}, \tag{7}$$

where η_s is the solvent viscosity. Using the constant for dextran, $K=49.3\times10^{-3}$ ml/g and $\alpha=0.60$ [28], we find $R_h=0.8$ nm and $D=2.9\times10^{-6}$ cm^2 s^{-1} for 3 kD dextran ($M_w=1500$) and $D=1.2\times10^{-6}$ cm^2 s^{-1} and $R_h=2.0$ nm for 10 kD dextran ($M_w=8800$).

Thus our observation that fluorescein ($R_h=0.4$ nm) can penetrate the fibrils easily and that the 10 kD dextran ($R_h=2$ nm) is excluded is consistent with existing estimates. Based on 10 kD dextran alone, we can place a clear upper bound on interstices of <4 nm. Since dextran samples are polydisperse and 3 kD dextran ($R_h=0.8$) is only partially excluded, this upper bound can be refined, our results suggest interstices are ~1.6 nm.

C. FRAP measurements

To characterize the mobility of our probes within the collagen fibrils, we monitored fluorescence recovery after photobleaching on single fibrils that were stained by immersion in fluorescein.

First, to characterize the radial diffusion coefficient $D_{\perp}$, a single fibril was bleached over a 50 μm length by moving

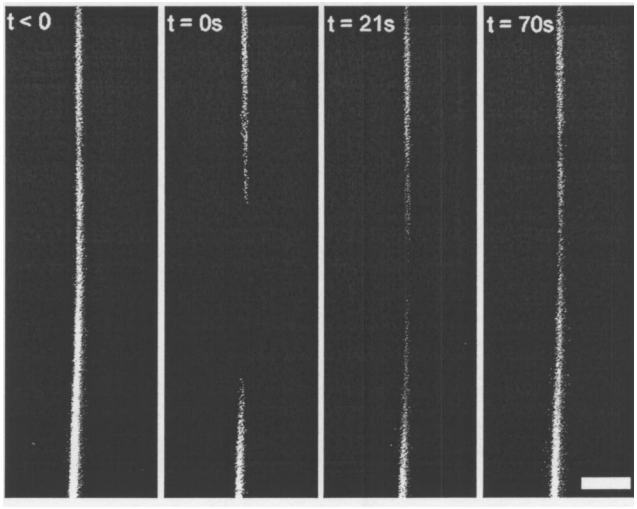

FIG. 6. Time series of fluorescence recovery observed with fluorescein in a collagen fibril. The fibril was bleached with the laser beam, and recovery of its intensity was monitored with the arc lamp. $t=0$ s is the first frame captured after the bleach. The scale bar is 2 μm.

the microscope stage to translate the fibril through the beam. In this manner, axial flux of dye was minimized. Fluorescence intensity along the fibril axis recovered homogeneously. When recovery was observed using full field epi-illumination from an arc lamp, no intensity gradients were detected.

Then, to characterize the axial diffusion coefficient $D_{\parallel}$, a similar fibril was bleached with a stationary laser spot ($\sim$5 μm). When observed in full field epi-illumination, the bleach spot brightened first at the edges and then in the center (Fig. 6). However, the times derived from the recovery curves were not measurably different from those obtained when the bleached area was 10 times larger.

We therefore conclude that, due to the fibril's small diameter ($<$500 nm), recovery is the result of fluorescent molecules diffusing into and out of the fibril radially. The impression of axial diffusion in full field (Fig. 6) is a likely result of the Gaussian profile of the bleaching spot. Since more molecules are bleached in the center than at the edges of the spot, complete recovery takes longer in the center.

For the recovery time to be sensitive to axial diffusion, the length of the bleached region must be such that the axial flux of molecules is greater than the radial flux. This might be achieved by making the extent of the bleached region less than the width of the fibril. However, since the width of a fibril is nearly equal to the wavelength of the light used for bleaching, such an experiment would be very difficult and was not possible with our setup.

Fluorescence recovery in a single fibril is then as follows: unbleached dye molecules diffuse from solution onto the fibril surface, are adsorbed and eventually diffuse into the fibril, repeatedly colliding with, binding to, and dissociating from collagen molecules. The extreme aspect ratio of the fibrils also results in the laser spot extending beyond the fibril diameter and bleaching probes in the surrounding solution. However, the presence of bleached probes in solution can be neglected since free diffusion is several orders of magnitude faster in solution than in a fibril (see below).

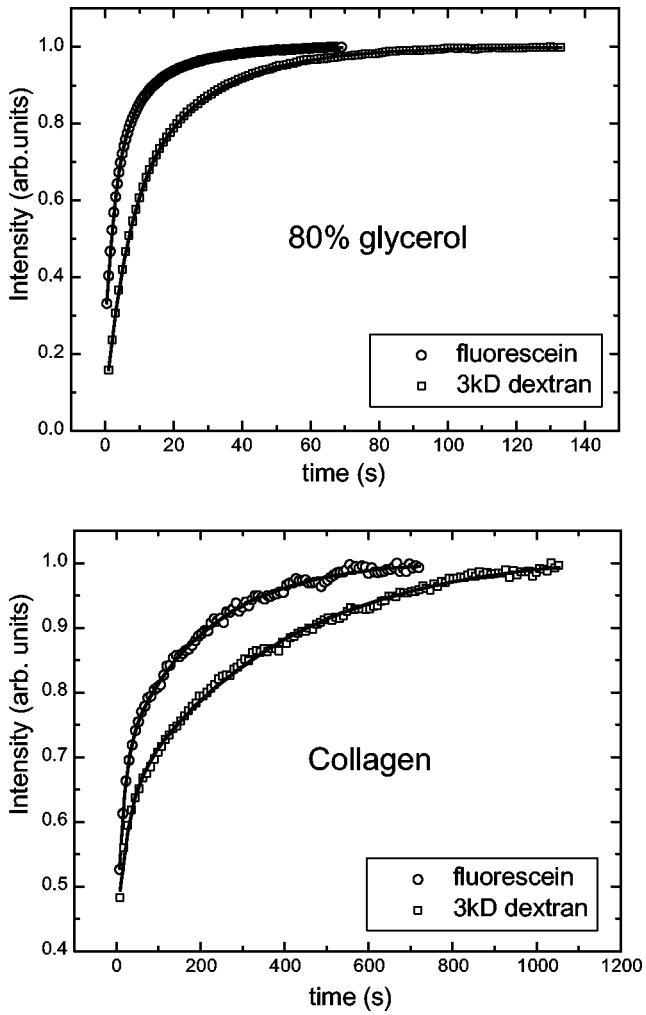

FIG. 7. Recovery curves for fluorescein and 3 kD dextran is glycerol and in collagen fibrils. Each point corresponds to the intensity integrated over the beam spot on one image. Lines are biexponential fits.

D. Comparison of recovery times

Radial diffusion in collagen was measured by bleaching stained fibrils over 5 μm as described in Sec. II B. Two dyes of different size were used (fluorescein and 3 kD fluoresceinated dextran). Their diffusion coefficients in glycerol solution were also determined and serve to calibrate our technique. The values obtained are very reproducible.

In glycerol and in fibrils, data are best fit with a biexponential function (Fig. 7). Recovery times were derived from both biexponential fits and from Eq. (1). By either measure, fluorescein diffuses twice as fast in free solution as 3 kD dextran (column 1, Table I), consistent with the respective hydrodynamic radii of the two molecules.

Measurements on collagen fibrils (column 2, Table I) showed a larger dispersion (15%–20%), presumably due to an unresolvable diversity of fibril diameters. Overall, 3 kD

TABLE I. Times obtained from the fits of the experimental curves with biexponential and Eq. (1) for the diffusion of dyes in collagen fibrils. t_1 is the long time from the biexponential fit and t_2 the short one. Each value is a mean over 11 measurements. Time ratios in column 3 were resealed to take into account the different geometry (see text). Times are in seconds.

	80% Glycerol			Fibrils			Fibril/glycerol	
	Times			Times			Ratio	
	Dextran	Fluorescein	Ratio	Dextran	Fluorescein	Ratio	Dextran	Fluorescein
t_1	26.4±2.3	13.2±0.7	2.0±0.3	273±27	130±17	2.1±0.5	1030±190	980±180
t_2	6.5±0.6	2.9±0.1	2.2±0.3	20±3	12±3	1.7±0.7	310±70	410±120
$t_{1/2}$	5.6±0.3	2.8±0.2	2.0±0.3	59±12	21±4	2.8±1.1	1050±270	750±200

dextran diffuses in fibrils ~2.4 times slower than fluorescein. Since both dyes have the same affinity for collagen in solution, we conclude that this effect is a result of the difference in the size of the probes. Without knowing the size distribution of the 3 kD dextran that actually permeated the fibril, we can still conclude that it included molecules greater than the size of interstices between collagen molecules in the fibril (~1.5 nm).

Note that both in fibrils and in glycerol, the bleached area is a cylinder and recovery is due to radial diffusion. In glycerol, images were taken in the plane of $D_\perp$, whereas in collagen, images were taken in the plane of $D_\parallel$. In glycerol, the bleached region is the size of the spot (5 μm), but in collagen it is only 0.5 μm (the diameter of fibrils). To compare recovery times in the two environments, it is therefore necessary to rescale according to the radial dimension of the bleached region.

Diffusion in fibrils is approximately 950 slower than in 80% glycerol (column 3, Table I), which is in turn 60 times slower than in water. The hydrodynamic radius of fluorescein is 0.4 nm, which yields a diffusion coefficient in water of 5.9×10^{-6} cm^2 s^{-1}. From our measurements, we can therefore deduce a diffusion coefficient in collagen fibrils $(1.0\pm0.2)\times10^{-10}$ cm^2 s^{-1}. For comparison, Song *et al.* [19] measured the diffusion of fluorescein into a synthetic polymer fibril (nylon 66) and obtained $D=(6.9\pm1.0)\times10^{-11}$ cm^2 s^{-1}.

Diffusion of probes in collagen gel has been measured under a variety of conditions [29–31]. The ratio of diffusion in 45 mg/ml succinylated collagen gel to that in water is 0.27 for anionic dextran ($M_w=69\,000$) [29]. In 50 mg/ml collagen gel, the ratio is 0.17 for FITC-dextran ($M_w=2900$) [30]. Values of D/D_0 ranging from 0.05 to 0.5 were reported in 45 mg/ml (type I) collagen gels for probes with size varying roughly from 1 to 20 nm [30]. These values are all three to four orders of magnitude higher than the values we measured.

The difference in density between collagen gels (50 mg/ml) and collagen fibrils (1200 mg/ml) alone cannot account for such a decrease, especially since fluorescein is smaller than the size of interstices in both cases. Thus binding effects are probably dominant for our measurements in fibrils. Binding was not an issue in the studies listed above because they were performed under conditions where collagen was completely saturated with dye and the vast majority of molecules detected would have been unbound.

We estimated the concentration of probe in our fibrils from the intensity recorded by the CCD camera under laser illumination. For fluorescein, this concentration was about 60 μM. This means that collagen in the fibrils (at an effective concentration of about 4 mM) are far from being saturated with probe—more than 98% of binding sites were empty at any time. Mobility is decreased by the presence of multiple adsorption sites and geometric obstacles. The five orders of magnitude difference is a result of repeated binding and unbinding events.

As can be seen in Fig. 4, fibrils also differ in shape (kinks, ends). The model proposed by Gutsmann *et al.* [17] stresses that the outer shell of a fibril is ''hard'' (e.g., cross-linked) whereas the inner region is ''soft.'' Kinks are then particular locations where the outer shell is weakened. If the outer shell presents a significant barrier to diffusion, one might expect the recovery to be faster in the vicinity of kinks. We found that the average recovery time obtained from measurements on regions containing kinks was not significantly faster (data not shown). We note, however, that the kinked region represents only a small proportion (15%) of the bleached region. Therefore, an effect would only be noticeable if the resistance of the shell must be comparably larger than the resistance of the core.

IV. CONCLUSION

Fluoresceinated molecules associate, dissociate, and diffuse in collagen fibrils. Using a simple experimental setup, we measured dye mobility in these biological fibers, which are less than 0.5 μm in diameter. Size exclusion effects yield an estimated pore size that agrees with previous structural measurements. FRAP measurements indicate a radial diffusion constant five orders of magnitude smaller than in free solution. The binding between fluorescein and collagen molecules has a $K_D\sim2$ μM. Although strong, it was necessary to work with background concentrations of fluorescent molecules in solution at least two orders of magnitude lower than K_D to achieve contrast. As a result, measurements on fibrils took place in the presence of a high density of open binding sites. We therefore suspect that repeated binding events account for most of the effect on diffusion.

It might be possible, with FRAP, to measure diffusion without binding in fibrils if a dye with less affinity for collagen were used. However, since fibril contrast depends on dye affinity, this would require a more sensitive apparatus than ours, to discriminate the recovery signal from the background.

On a general level, this study provides experimental data on the diffusion of molecules (gas, impurities, etc.) in a cylindrical fiber with a high density of adsorption sites (optical fibers, polymer fibers, etc.) that could be compared to numerical simulations [32]. An investigation of transport anisotropy along collagen fibrils, one of the inspirations for this effort, remains a challenge because the aspect ratio and surface chemistry of the fibrils makes it very difficult to minimize the radial flux.

ACKNOWLEDGMENTS

We thank P. K. Hansma for inspiration and fruitful discussions and Diane McClure for providing a supply of rat tails. This work was supported partially by the National Science Foundation, through the CAREER program under Award No. 9985493 and through the MRL Program under Award No. DMR00-80034, and partially by the Alfred P. Sloan Foundation (D.K.F.).

[1] A. L. Boskey, T. M. Wright, and R. D. Blank, J. Bone Miner. Res. **3**, 330 (1999).
[2] P. Fratzl, K. Misof, I. Zizak, G. Rapp, H. Amenitsch, and S. Bernstorff, J. Struct. Biol. **122**, 119 (1998).
[3] E. M. Culav, C. H. Clark, and M. J. Merrilees, Phys. Ther. **79**, 308 (1999).
[4] A. Miller, in *Biochemistry of Collagen*, edited by G. N. Ramachandran and A. H. Reddi (Plenum, New York, 1976).
[5] D. A. D. Parry and A. S. Craig, in *Ultrastructure of the Connective Tissue Matrix*, edited by A. Ruggeri and P. M. Motta (Martinus Nijhoff, Boston, 1984).
[6] A. J. Hodge and J. A. Petruska, in *Aspects of Protein Structure*, edited by G. N. Ramachandran (Academic, New York, 1963).
[7] J. A. Chapman and D. J. S. Hulmes, in *Ultrastructure of the Connective Tissue Matrix*, edited by A. Ruggeri and P. M. Motta (Martinus Nijhoff, Boston, 1984).
[8] R. D. B. Fraser, T. P. MacRae, and A. Miller, J. Mol. Biol. **193**, 115 (1987).
[9] M. Raspanti, T. Congiu, and S. Guizzardi, Matrix Biol. **20**, 601 (2001).
[10] A. Bigi, M. Gandolfi, N. Roveri, and G. Valdre, Biomaterials **18**, 657 (1997).
[11] D. J. S. Hulmes and A. Miller, Nature (London) **282**, 878 (1979).
[12] D. J. S. Hulmes, D. F. Holmes, and C. Cummings, J. Mol. Biol. **184**, 473 (1985).
[13] P. Fratzl, N. Fratzl-Zelman, and K. Klaushofer, Biophys. J. **64**, 260 (1993).
[14] D. J. S. Hulmes, T. J. Wess, D. J. Prockop, and P. Fratzl, Biophys. J. **68**, 1661 (1995).
[15] D. J. Prockop, and A. Fertala, J. Struct. Biol. **122**, 111 (1998).
[16] R. I. Price, S. Lees, and D. A. X. Kirchner, Int. J. Biol. Macromol. **20**, 23 (1997).
[17] T. Gutsmann, G. E. Fantner, M. Venturoni, A. Ekani-Nkodo, J. B. Thompson, J. H. Kindt, D. E. Morse, D. K. Fygenson, and P. K. Hansma, Biophys. J. (in press).
[18] I. D. Rattee and S. So, J. Membr. Sci. **15**, 171 (1983).
[19] Y. Song, M. Srinivarasao, A. Tonelli, C. M. Balik, and R. McGregor, Macromolecules **33**, 4478 (2000).
[20] S. Papadopoulos, K. D. Jürgens, and G. Gros, Biophys. J. **79**, 2084 (2000).
[21] J. L. Ross and D. K. Fygenson, Biophys. J. (in press).
[22] *CRC Handbook of Chemistry and Physics*, 68th ed., edited by R. C. Weast (CRC Press, Boca Raton, 1987).
[23] R. Swaminathan, C. P. Hoang, and A. S. Verkman, Biophys. J. **72**, 1900 (1997).
[24] H. P. Kao, J. R. Abney, and A. S. Verkman, J. Cell Biol. **120**, 175 (1993).
[25] D. Axelrod, D. E. Koppel, J. S. Schlessinger, E. Elson, and W. W. Webb, Biophys. J. **16**, 1055 (1976).
[26] P.-G. de Gennes, *Scaling Concepts in Polymer Physics* (Cornell University Press, Ithaca, 1979).
[27] Y. Oono and M. Kohmoto, J. Chem. Phys. **78**, 520 (1983).
[28] *Polymer Handbook*, 4th ed., edited by J. Brandrup, E. H. Immergut, and E. A. Grulke (Wiley, New York, 1999).
[29] V. Shenoy and J. Rosenblatt, Macromolecules **28**, 8751 (1995).
[30] M. Shaw and A. Schy, Biophys. J. **34**, 375 (1981).
[31] S. Ramanujan, A. Pluen, T. D. McKee, E. B. Brown, Y. Boucher, and R. K. Jain, Biophys. J. **84**, 1650 (2002).
[32] F. Weling, J. Appl. Phys. **58**, 1493 (1985).